Applied Physics A (2020) 126:502
https://doi.org/10.1007/s00339-020-03697-x

Applied Physics A
Materials Science & Processing

(59.5–*x*) P_2O_5–30Na_2O–10Al_2O_3–0.5CoO–*x*Nd_2O_3 glassy system: an experimental investigation on structural and gamma-ray shielding properties

Reda Elsaman[1] · Shams A. M. Issa[1,2] · H. O. Tekin[3] · G. Susoy[4] · A. A. Showahy[1] · M. M. Elokr[5] · T. T. Erguzel[6] · Yasser B. Saddeek[1,7]

Received: 8 April 2020 / Accepted: 2 June 2020 / Published online: 9 June 2020

Abstract
In this study, five different glasses encoded ND1, ND2, ND3, ND4 and ND5 based on (59.5–*x*) P_2O_5–30Na_2O–10Al_2O_3–0.5CoO–*x*Nd_2O_3 (*x* = 1, 2, 3, 4 and 5 mol%) glass system were fabricated. Using two γ- ray energies emitted from point sources, 356 keV (^{133}Ba) and 662 keV (^{137}Cs), γ-ray attenuation coefficients were measured as a function of the Nd_2O_3 concentration. The theoretical values of the mass attenuation coefficient were calculated using the XCOM program at 0.015–15-MeV photon energies. As it is underlined in the results section, the mass attenuation coefficient increases as the Nd_2O_3 concentration increases. X-ray diffraction (XRD) was characterized for fabricated glasses. Moreover, different shielding parameters such as half-value layer (HVL), mean free path (MFP), effective atomic numbers (Z_{eff}), basic gamma-ray attenuation properties such as exposure buildup factors (EBF) and energy absorption buildup factors (EABF) at different penetration depths were calculated. With increasing Nd_2O_3 additive in glass samples, half-value layer (HVL), average free path (MFP), exposure and energy absorption buildup factor (EBF and EABF) values decrease. On the other hand, Z_{eff} values increase with increasing Nd_2O_3 additive in glass samples at the photon energy 0.015–15 MeV. The results highlighted that ND5 sample with highest value of Nd_2O_3 (5 mol%) showed excellent nuclear radiation shielding properties.

Keywords XRD · Nd_2O_3 · Glass · Shielding

1 Introduction

Ionizing radiation is an important term to be considered along with its benefits and potential risks. Despite its benefits in medical diagnosis and treatment practices, the risk status on living biological structures should always be considered and minimized. Gamma radiation shielding is a very important application because γ-rays have risky effect on human health. The ALARA principle suggests the use of the most suitable shielding material to reduce the amount of ionized radiation exposed. Technological developments have brought with the use of new methods for radiation shielding studies. Moreover, the development and use of radiation shielding materials that are environmentally friendly, low cost and have high material durability is one of the most popular research topics in the literature in recent years. Glass materials which are new and promising material types in terms of structural development, transparency, high durability and environmental friendliness features used for radiation shielding have gained a very useful place in nuclear reactors,

✉ H. O. Tekin
tekin765@gmail.com

[1] Physics Department, Faculty of Science, Al-Azhar University, Assiut 71452, Egypt

[2] Department of Physics, Faculty of Science, University of Tabuk, Tabuk, Saudi Arabia

[3] Medical Diagnostic Imaging Department, College of Health Sciences, University of Sharjah, 27272 Sharjah, United Arab Emirates

[4] Department of Physics, Faculty of Science, Istanbul University, 34134 Istanbul, Turkey

[5] Physics Department, Faculty of Science, Al-Azhar University, Cario, Egypt

[6] Department of Software Engineering, Faculty of Engineering and Natural Sciences, Uskudar University, 34672 Istanbul, Turkey

[7] Physics Department, College of Science in Zulfi, Majmaah University, Al Majma'ah 11952, Saudi Arabia

fusion reactors and modern accelerator technology. As it is clearly seen from the previous studies, lead (Pb) materials which have various disadvantages to protect against gamma rays have been replaced by various types of materials such as concrete and glass to protect them from gamma rays [1–3]. Glass materials [4–8] are a very reliable material used in radiation shielding instead of concrete [9–11]. Various phosphate glass systems (PG) with characteristics such as low dispersion power, low refractive index, high gain density, low melting point and high thermal stability are being developed day by day by combining glass-forming oxides (SiO_2 and TeO_2) and modifying oxides (Al_2O_3, CaO, K_2O, PbO, Na_2O, BaO, MgO, CaF_2, Fe_2O_3, ZnO, TiO_2, etc.). By adapting the chemical mixtures of phosphate-based glass structures, it can be quite suitable material types which can be manufactured for different functional applications.

The addition of Al_2O_3 to phosphate-based glass samples has the effect of increasing cross-links between PO_4 units that form Al–O–P bonds. These Al–O–P bonds are more covalent than P–O–P bonds. On the other hand, P–O–P bonds have a straight impact on some characteristic features [chemical resistance, glass transition temperature (T_g), density and thermal expansion coefficient (α)] of glass samples. In addition, as alkali metal oxide (e.g., Na_2O) is added to the glass materials, it causes the P–O–P bonds to break, the three-dimensional networks turn into linear phosphate chains and the formation of NBOs consisting of P–O–Na (K) bonds that are weaker than P–O–Al bonds. CoO, added to glass materials, has a positive effect due to its easy processing, stability at high temperatures and adjustable release kinetics [12–24]. In this paper, five different glasses based on (59.5–x) P_2O_5–30Na_2O–10Al_2O_3–0.5CoO–$x$$Nd_2O_3$ system were examined in terms of structural and gamma ray shielding properties. To examine the shielding properties of the materials, the most basic parameter used is the mass attenuation coefficient (μ_m). The attenuation principle of photons is interpreted in three different processes. The first of these interaction processes are photoelectric absorption, which is effective in low energies; the second is Compton scattering, which is effective in medium energies; and lastly pair production that is active in high energies. The total value of the mass attenuation coefficient is equal to the sum of these three processes and is related by the primary energy of the photon, average atomic number (Z) and chemical system of the substance [25, 26]. In this study, five different glasses encoded ND1, ND2, ND3, ND4 and ND5 based on (59.5–x) P_2O_5–30Na_2O–10Al_2O_3–0.5CoO–$x$$Nd_2O_3$, where $x = 1, 2, 3, 4$ and 5 (mol%) glass system, were fabricated. In addition, X-ray powder diffraction (XRD) was utilized for structural analyses. Next, an experimental gamma-ray transmission setup was established for calculation of mass attenuation coefficients of fabricated glasses. We used 0.356- and 0.662-MeV gamma photons energies emitted from point isotropic gamma sources, namely ^{133}Ba and ^{137}C. It is worth to mention that this study aimed to observe the total impact of P_2O_5 replacement by Nd_2O_3. Therefore, the hypothesis of recent investigation can be highlighted by Nd_2O_3 reinforce effect and multiple impact on structural and gamma-ray attenuation properties of fabricated glasses. To provide the infrastructure of this hypothesis, Al_20_5, Na_2O and CoO ratios were kept constant and the effect of Nd_2O_3 ratio, which increased with partial decrease of P_2O_5 ratio (Table 1), was investigated. On the other hand, the theoretical mass attenuation coefficient values were examined using the XCOM program at 356-keV and 662-keV photon energy values. X-ray diffraction (XRD) was characterized for fabricated glasses. The investigated properties of novel glasses can be listed as follows:

- X-ray powder diffraction (XRD) of fabricated glasses.
- Half-value layer (HVL), mean free path (MFP).
- Effective atomic numbers (Z_{eff}).
- Exposure buildup factors (EBF) and energy absorption buildup factors (EABF) at different penetration depths have been calculated at different Nd_2O_3 mol% levels and the energies (0.015–15 MeV).
- A comprehensive mass attenuation coefficient investigation.

The data achieved from this study can be useful for further research on the use of glass materials, a new generation material, in efficient and environmentally friendly shielding applications. The hypothesis of this research is to evaluate the multiple effects of increasing Nd_2O_3 additive amount on structural and ionizing radiation attenuation features of fabricated glass samples. Therefore, outcomes from recent investigation will be discussed in terms of increased

Table 1 Samples codes, elemental compositions and density (ρ) of glass samples

Code	O	Na	Al	P	Co	Nd	ρ (g/cm^2)
ND1	0.456706	0.222557	0.052925	0.255306	0.003932	0.008574	2.645
ND2	0.452496	0.222557	0.052925	0.250942	0.003932	0.017148	2.665
ND3	0.448287	0.222557	0.052925	0.246578	0.003932	0.025721	2.753
ND4	0.444078	0.222557	0.052925	0.242214	0.003932	0.034294	2.83
ND5	0.439868	0.222557	0.052925	0.237849	0.003932	0.042869	2.868

Nd_2O_3 additive amount in manufactured glass samples. The obtained results from this experimental investigation can be useful for new approaches on novel, efficient and eco-friendly glass shields and their utilization for different types of ionizing radiation facilities such as medical radiation facilities, industrial radiation areas and research laboratories.

2 Materials and methods

Glass samples with chemical formula (59.5–x) P_2O_5–30Na_2O–10Al_2O_3–0.5CoO–xNd_2O_3, where $x = 1$, 2, 3, 4, mol%). were prepared by the conventional melt quenching method and are given in Table 1. The materials that initiate the reaction are reagent grade $(NH_4)_2HPO_4$, Na_2CO_3, Al_2O_3, CoO and Nd_2O_3. Powdered oxides were melted at 1050–1150 °C in a porcelain vessel in an air-conditioned electric oven for 35–45 min. To ensure homogeneity, melt shaking was performed during the preparation phase. Samples prepared by pouring the melt into preheated molds at 350 °C were left to anneal for a few hours at 450 °C. The oven was then left to cool to room temperature. The prepared samples were then ground and polished for XRD. XRD is often used to verify the glassy structure of the samples. When no peak is observed in the patterns obtained as a result of verification, the amorphous structure of the samples examined is verified. Gamma-ray shielding parameters of glass samples were measured using 0.356-MeV and 0.662-MeV gamma photons, which were emitted from point sources of ^{133}Ba and ^{137}Cs. The mass attenuation coefficients (μ_m) of the samples were evaluated using the NaI (T1) scintillation detector with the setup scheme depicted in Fig. 1. Some of the features of this detector are: Gammas of 0.662 MeV, emitted from ^{137}Cs point source, have a 7.5% resolution and the thickness of the Al window is 0.5 mm. The measurement time for each sample was approximately 4 h and the measurement were repeated three times. Finally, densities of glasses have been determined with well-known Archimedes method. We remark that the measurement was repeated three times on each sample.

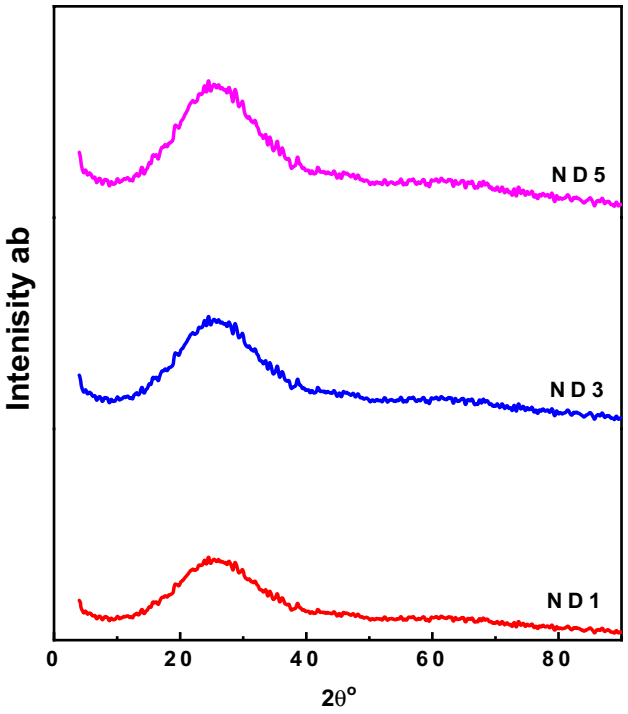

Fig. 2 X-ray diffraction (XRD) patterns for glass samples

3 Theory

If the absorbent material is a chemical mixture or compound, the mass attenuation coefficient (μ_m) is estimated by the mixture rule and is expressed as given in the equation below [27, 28]:

$$\mu_m = \sum_i w_i(\mu_m)_i. \quad (1)$$

Here, w_i is partial mass component of the ith element in the investigated glass sample. In our work, the $_m$ results of glass samples were obtained using the theoretical XCOM program. By the help of $_m$ values, other shielding terms such as transmission factors (e.g., HVL, MFP) were then calculated by employing the equations as follows:

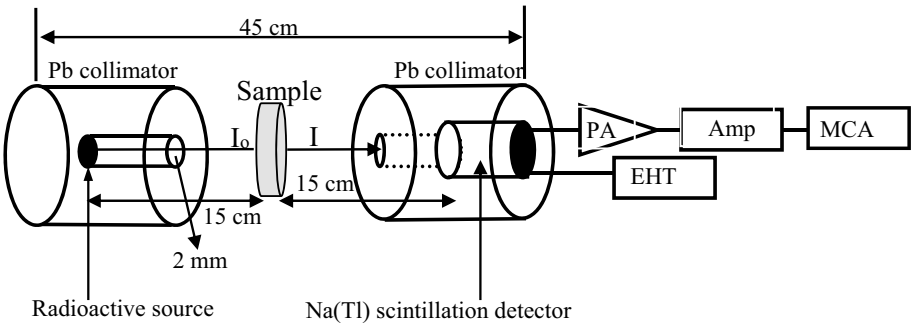

Fig. 1 Narrow beam geometrical setup

Table 2 Experimental and theoretical mass attenuation with their relative difference (Δ) of glass samples

E (MeV)	ND1	ND2	ND3	ND4	ND5
0.356					
XCOM	0.098260	0.098730	0.099200	0.099670	0.100100
This work	0.098855	0.098535	0.098936	0.100133	0.102293
Δ	0.61	0.20	0.27	0.46	2.19
0.662					
XCOM	0.075610	0.075640	0.075660	0.075690	0.075720
This work	0.075180	0.075596	0.075986	0.076262	0.085051
Δ	0.06	0.43	0.76	12.32	0.57

$$\Delta = \frac{\text{XCOM}-\text{Experimental}}{\text{XCOM}} \times 100$$

$$\text{HVL} = \frac{\text{Ln}(2)}{\mu}, \tag{2}$$

$$\text{MFP} = \frac{1}{\mu}. \tag{3}$$

Z_{eff} values of fabricated glass samples were determined by the help of Eq. 4 [29–31]:

$$Z_{\text{eff}} = \frac{\sum_i f_i A_i \left(\frac{\mu}{\rho}\right)_i}{\sum_j f_j \frac{A_j}{Z_j} \left(\frac{\mu}{\rho}\right)_j}. \tag{4}$$

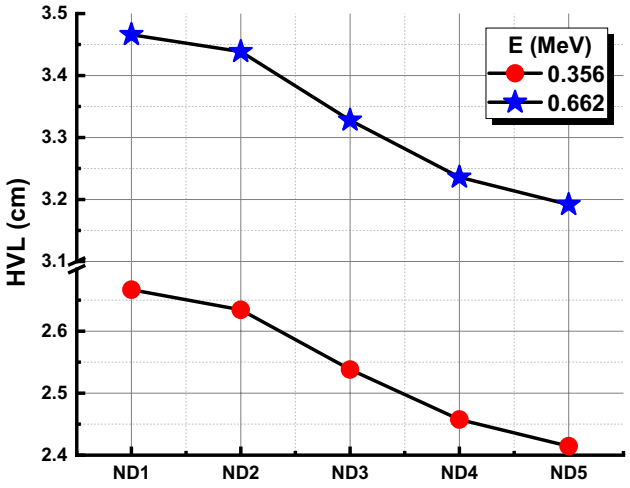

Fig. 4 Half-value layer (HVL) results as a function of glass samples

In the formula, f_i, μ, Z_i and A_i indicate the fraction of each element, linear attenuation coefficient, atomic number and atomic weight, respectively. The equivalent atomic number (Z_{eq}) values for the prepared glass samples were estimated using the equation given below [32–34].

$$Z_{\text{eq}} = \frac{Z_1\left(\log R_2 - \log R\right) + Z_2(\log R - \log R_1)}{\log R_2 - \log R_1}. \tag{5}$$

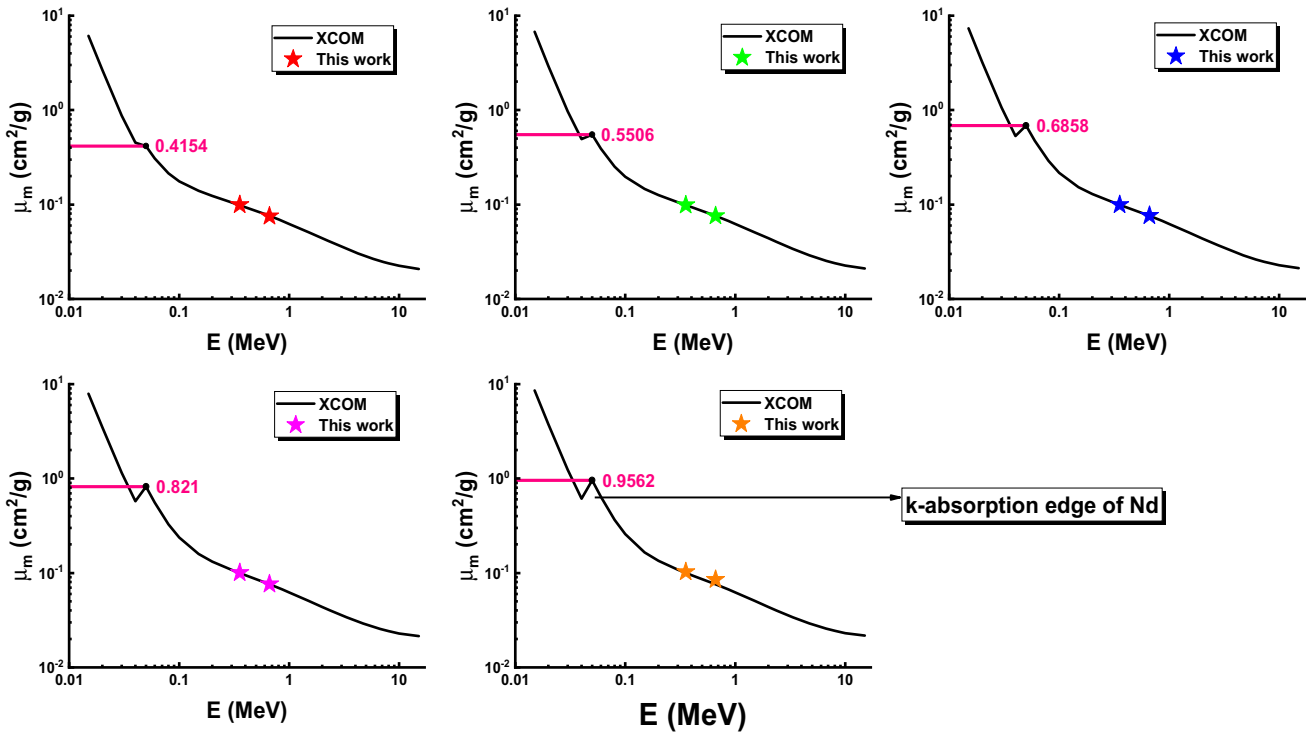

Fig. 3 Mass attenuation coefficient (μ_{m}) values as a function of photon energy glass samples

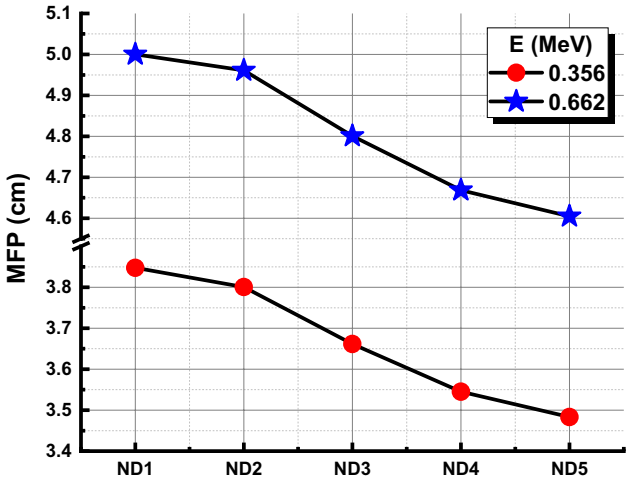

Fig. 5 Mean free path (MFP) values as a function of glass samples

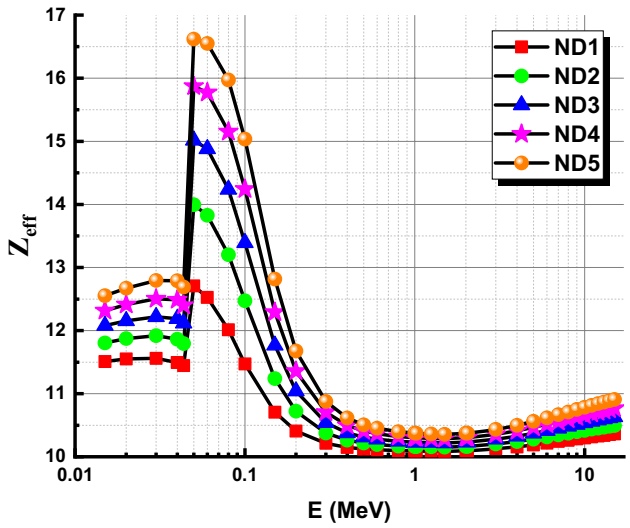

Fig. 6 Effective atomic number (Z_{eff}) values as a function of photon energy glass samples

The terms of EBF and EABF give successful information about the number of photons, intensity, energy flux, and dose. Recently, EBF and EABF of ND1, ND2, ND3, ND4 and ND5 based on (59.5–*x*) P_2O_5–30Na_2O–10Al_2O_3–0.5CoO–xNd_2O_3, where *x* = 1, 2, 3, 4 and 5 (mol%), were determined for gamma energies up to 15 MeV and for penetration depth up to 40 MFP using G-P fitting method. To estimate the buildup factors of fabricated glass samples, the equivalent atomic numbers (Z_{eq}) are first determined. The Z_{eq} can be determined based on the following interpolation equation [35–37]:

$$Z_{\text{eq}} = \frac{Z_1\left(\log R_2 - \log R\right) + Z_2\left(\log R - \log R_1\right)}{\log R_2 - \log R_1}, \tag{6}$$

$$C = \frac{C_1\left(\log Z_2 - \log Z_{eq}\right) + C_2(\log Z_{\text{eq}} - \log Z_1)}{\log Z_2 - \log Z_1}, \tag{7}$$

$$B(E,X) = 1 + \left(\frac{b-1}{K-1}\right)(K^x - 1), \text{for} K \neq 1 \tag{8}$$

$$B(E,X) = 1 + (b-1)x, \text{for} K = 1 \tag{9}$$

where

$$K(E,x) = cx^a + d\frac{\tanh\left(\frac{x}{X_K} - 2\right) - \tanh(-2)}{1 - \tanh(-2)} \quad \text{for } x \leq 40\text{mfp}. \tag{10}$$

Here, *R* is the ratio between Compton-attenuation and total attenuation ($(\mu/\rho)_{\text{Comp}}/(\mu/\rho)_{\text{total}}$). The next step is to obtain G-P fitting parameters using Z_{eq} values utilizing the Eq. 8. Finally, the buildup factors of fabricated glasses were studied. These equations contain *x* as the distance between the source and the detector. At 1 mfp, the EBF is coded by *b*. *K*(*E*, *X*) factor has a meaning of dose multiplication [38, 39].

4 Results and discussion

4.1 XRD analysis

To initiate XRD measurement and verify the glassy structure of the samples, three of the powder samples were selected and shown in Fig. 2. As can be clearly seen from Fig. 2, a bump structure was observed at 15°–35° in all three examples; while, diffraction peaks confirming the non-crystalline glass structure of the prepared samples were not observed.

4.2 Radiation shielding parameters

High-density glass samples have larger atomic numbers and can be considered an effective material for the gamma-ray shielding. This is related to the chemical composition of the glasses as well as the commitment to photon energy. The experimental and theoretically (XCOM) calculated mass attenuation coefficients (μ_m) of glass samples prepared at 0.356- and 0.662-MeV gamma photons emitted from spot sources ^{133}Ba and ^{137}C can be seen from Table 2. According to Table 2, the μ_m values in the 0.356 MeV and 0.662 MeV energy increase with increasing Nd_2O_3 contribution (i.e.,

Table 3 (EBF and EABF) G-P fitting coefficients (b, c, a, X_k and d) of ND1 glass sample

E (MeV)	Z_{eq}	EBF					EABF				
		b	c	a	X_k	d	b	c	a	X_k	d
0.015	11.96	1.0375	0.4003	0.2114	13.2742	− 0.1326	1.0375	0.3888	0.2105	13.2657	− 0.1318
0.020	12.07	1.0838	0.4353	0.1809	14.3040	− 0.0930	1.0860	0.4208	0.1888	14.1568	− 0.0968
0.030	12.20	1.2748	0.4435	0.1908	14.5258	− 0.1024	1.2802	0.4389	0.1940	14.2195	− 0.1033
0.040	12.29	1.5761	0.5409	0.1499	15.0536	− 0.0798	1.6022	0.5376	0.1510	15.1668	− 0.0806
0.050	14.48	1.5881	0.5504	0.1481	14.9115	− 0.0805	1.6266	0.5657	0.1369	16.0693	− 0.0716
0.060	14.72	1.7904	0.6520	0.1101	14.9207	− 0.0602	2.0375	0.5540	0.1600	21.9350	− 0.0847
0.080	15.06	2.1882	0.7574	0.0833	13.0704	− 0.0511	2.7513	0.7208	0.0980	13.4955	− 0.0666
0.100	15.31	2.3833	0.9169	0.0374	13.7232	− 0.0415	3.3637	0.8974	0.0437	13.6611	− 0.0450
0.150	15.73	2.5239	1.1504	− 0.0175	12.3534	− 0.0180	3.8656	1.1891	− 0.0281	14.7887	− 0.0078
0.200	16.06	2.4951	1.2660	− 0.0384	11.0052	− 0.0125	3.6774	1.3345	− 0.0551	19.4767	0.0048
0.300	16.62	2.3723	1.3473	− 0.0534	8.2161	− 0.0101	3.1542	1.4425	− 0.0755	17.8223	0.0170
0.400	16.67	2.2674	1.3910	− 0.0651	16.2355	0.0070	2.8362	1.4580	− 0.0792	16.8439	0.0178
0.500	16.75	2.1791	1.4005	− 0.0703	18.6147	0.0160	2.6053	1.4563	− 0.0811	16.1470	0.0204
0.600	16.90	2.1132	1.3813	− 0.0681	18.4540	0.0155	2.4496	1.4341	− 0.0788	16.3153	0.0210
0.800	16.90	2.0128	1.3475	− 0.0651	16.5669	0.0166	2.2502	1.3858	− 0.0732	15.5141	0.0214
1.000	16.88	1.9391	1.3084	− 0.0601	15.9321	0.0170	2.1245	1.3318	− 0.0660	15.3055	0.0209
1.500	13.53	1.8480	1.2300	− 0.0480	15.5306	0.0166	1.9405	1.2428	− 0.0515	14.5369	0.0190
2.000	11.52	1.7908	1.1545	− 0.0335	15.3215	0.0115	1.8392	1.1598	− 0.0351	14.5749	0.0128
3.000	11.28	1.6811	1.0583	− 0.0042	12.1870	0.0000	1.7031	1.0531	− 0.0099	11.8165	− 0.0007
4.000	11.16	1.6047	0.9928	0.0058	12.8864	− 0.0089	1.6128	0.9845	0.0085	13.3743	− 0.0116
5.000	11.16	1.5363	0.9535	0.0173	14.3733	− 0.0207	1.5432	0.9421	0.0206	12.7275	− 0.0170
6.000	11.12	1.4927	0.9166	0.0301	11.4603	− 0.0240	1.4784	0.9290	0.0241	15.8999	− 0.0273
8.000	11.13	1.4059	0.9020	0.0331	13.5730	− 0.0263	1.3869	0.9038	0.0329	12.2370	− 0.0233
10.000	11.09	1.3465	0.8770	0.0428	13.1803	− 0.0335	1.3225	0.8963	0.0353	13.9920	− 0.0282
15.000	11.10	1.2620	0.8254	0.0633	14.3389	− 0.0557	1.2256	0.8872	0.0400	14.6635	0.0242

when switching from ND1 glass sample to ND5 glass sample) [40]. The μ_m values are highest for the ND5 sample, while the lowest for the ND1 sample (see Table 2). This is because the ND5 sample contains the highest amount of Nd_2O_3 additives than other samples. The experimental results and XCOM results are slightly different underlining the performance of the model in terms of both robustness and high correlation with experimental outcomes. As can be seen also from Fig. 3, the experimental and theoretical data of μ_m values are highly compatible and supportive. As seen in Fig. 3, a peak is observed at 0.4154 MeV, 0.5506 MeV, 0.6858 MeV, 0.821 MeV and 0.9562 MeV due to the K absorption edge of the Nd element for glass samples of ND1, ND2, ND3, ND4 and ND5, respectively. As it is known, photons interact with the material in three ways and the sharp decrease in μ_m values in Fig. 3 is caused by the photoelectric event from these interaction processes [41–43]. Because the microscopic cross-section value is directly proportional to Z^{4-5} and inversely proportional to $E^{-3.5}$. While the change in μ_m values is quite low in medium energies where Compton scattering is effective, the μ_m values take almost constant value due to the dominant pair production in high energies [44, 45]. The effect of the Nd_2O_3 additive on the half-value layer (HVL) and the mean free path (MFP) measurement results in glass samples is shown in Figs. 4 and 5. As can be seen from the Figs. 4 and 5, these values decrease with increasing Nd_2O_3 contribution. On the other hand, when photon energy is high, HVL and MFP values are also high. The HVL, one of the well-known shielding parameters, is a shield or absorber that reduces the radiation level to half the original intensity. On the other hand, the MFP shows the average distance between two consecutive gamma photon interactions [45, 46]. These two concepts are quick and very practical in approximate shielding calculations. Therefore, HVL and MFP should be small to achieve a strong radiation shielding in glass samples means low HVL and MFP values indicate the best radiation shielding. That is, as the density values of the glass samples increase, the MFP and HVL values decrease [47]. Thus, the high density ND5 glass sample has the minimum value for these two measurements, i.e. ND5 glass sample is the best shielding material among the

Table 4 (EBF and EABF) G-P fitting coefficients (*b*, *c*, *a*, X_k and *d*) of ND2 glass sample

E (MeV)	Z_{eq}	EBF					EABF				
		b	*c*	*a*	X_k	*d*	*b*	*c*	*a*	X_k	*d*
0.015	12.32	1.0344	0.3987	0.2093	14.0512	− 0.1351	1.0344	0.3888	0.2206	13.5913	− 0.1455
0.020	12.45	1.0767	0.4136	0.1974	14.0950	− 0.1046	1.0801	0.3904	0.2109	14.1962	− 0.1100
0.030	12.62	1.2470	0.4320	0.1947	14.8347	− 0.1034	1.2511	0.4261	0.2005	14.1337	− 0.1086
0.040	12.75	1.5135	0.5162	0.1604	14.8753	− 0.0860	1.5382	0.5079	0.1647	14.9472	− 0.0898
0.050	16.30	1.4196	0.4783	0.1802	14.5491	− 0.1014	1.4537	0.4704	0.1830	14.6475	− 0.1025
0.060	16.65	1.5745	0.5530	0.1495	14.5354	− 0.0835	1.6617	0.5547	0.1448	15.3008	− 0.0792
0.080	17.12	1.8343	0.7011	0.0952	14.6119	− 0.0548	2.3026	0.5861	0.1512	13.3506	− 0.0927
0.100	17.46	2.0340	0.8279	0.0569	14.1184	− 0.0417	2.8348	0.7356	0.0949	13.3773	− 0.0702
0.150	18.06	2.2484	1.0379	0.0044	13.4181	− 0.0242	3.5491	1.0027	0.0151	13.4676	− 0.0314
0.200	18.44	2.2971	1.1710	− 0.0214	11.9932	− 0.0171	3.5678	1.1723	− 0.0212	12.4429	− 0.0179
0.300	18.95	2.2554	1.2836	− 0.0433	10.0899	− 0.0111	3.1866	1.3126	− 0.0488	9.8671	− 0.0087
0.400	19.14	2.2055	1.3127	− 0.0487	8.9870	− 0.0106	2.8411	1.3843	− 0.0662	21.0301	0.0138
0.500	19.32	2.1239	1.3426	− 0.0582	17.0004	0.0058	2.6231	1.3915	− 0.0690	17.3822	0.0140
0.600	19.48	2.0642	1.3433	− 0.0611	20.8522	0.0136	2.4661	1.3811	− 0.0686	18.6463	0.0172
0.800	19.65	1.9685	1.3241	− 0.0603	18.2689	0.0156	2.2601	1.3481	− 0.0653	16.4023	0.0168
1.000	19.73	1.9067	1.2898	− 0.0563	16.7752	0.0156	2.1287	1.3064	− 0.0595	16.1082	0.0166
1.500	14.66	1.8366	1.2273	− 0.0473	15.2812	0.0157	1.9423	1.2363	− 0.0497	14.7896	0.0174
2.000	12.14	1.7861	1.1547	− 0.0329	15.9945	0.0106	1.8341	1.1643	− 0.0357	14.4887	0.0127
3.000	11.74	1.6765	1.0620	0.0069	14.9602	− 0.0014	1.6985	1.0582	− 0.0112	13.7329	0.0000
4.000	11.55	1.6015	0.9948	0.0054	12.9490	− 0.0090	1.6101	0.9880	0.0073	13.8832	− 0.0105
5.000	11.51	1.5370	0.9481	0.0202	12.5647	− 0.0211	1.5457	0.9334	0.0242	12.8534	− 0.0215
6.000	11.48	1.4890	0.9239	0.0275	11.6922	− 0.0220	1.4765	0.9290	0.0245	15.6975	− 0.0278
8.000	11.45	1.4055	0.9020	0.0335	13.6764	− 0.0271	1.3843	0.9057	0.0325	12.1336	− 0.0232
10.000	11.42	1.3449	0.8803	0.0421	13.1471	− 0.0334	1.3176	0.9043	0.0330	14.2044	− 0.0270
15.000	11.43	1.2586	0.8336	0.0609	14.3012	− 0.0539	1.2277	0.8707	0.0469	14.4716	− 0.0047

glass samples. In composite materials, the effective atomic number and density values affect the absorption and scattering of photon interactions. Composite materials are very successful at reducing gamma rays when they have a higher effective mass number, since they will have more electrons per atom. The effective atomic number (Z_{eff}) values of the five glass samples were calculated using Eq. 4 in the energy region of 0.015–15 MeV and are shown in Fig. 6. As can be seen from the figure, Z_{eff} value decreases for all glass samples with the increase of photon energy. In addition, instant changes in Z_{eff} values are seen due to the K absorption edge. Also, the Z_{eff} values increases as the Nd_2O_3 increases from 1 to 5 mol%. The two other important gamma shielding parameters are exposure buildup factor (EBF) and energy absorption buildup factor (EABF). While EBF expresses the energy absorption properties of air, EABF describes the energy absorbed or accumulated in the attenuator. The calculated values of equivalent atom number (Z_{eq}), EBF and EABF are shown in Tables 3, 4, 5, 6 and 7, respectively, for glass samples ND1, ND2, ND3, ND4 and ND5.

Figures 7 and 8 show EBF and EABF changes for five different glass samples in the energy region of 0.015–15-MeV photon energy and at different penetration depths (1 mfp, 5 mfp, 10 mfp, 20 mfp and 40 mfp). As can be seen from Figs. 7 and 8, the minimum EBF and EABF values of the glass samples were observed at low energies. The reason for this is perhaps the photoelectric effect process [7, 48, 49]. EBF–EABF values increase with increasing energy in the middle energy region and reach a maximum of approximately at 0.6-MeV energy and then decrease with increasing energy value. This response can be associated with multiple scattering caused by Compton effect. In addition, EBF and EABF values increase with increasing penetration depth values for glass samples. On the other hand, in Figs. 9 and 10, the EBF and EABF values of all glass samples at a certain penetration depth value of 15 mfp are examined depending on the energy. While the EBF and EABF values of ND1 glass sample with the lowest Nd_2O_3 additive (1%) are highest, the EBF and EABF values of ND5 glass sample with the highest Nd2O3 additive (5%) are minimum.

Table 5 (EBF and EABF) G-P fitting coefficients (b, c, a, X_k and d) of ND3 glass sample

E (MeV)	Z_{eq}	EBF					EABF				
		b	c	a	X_k	d	b	c	a	X_k	d
0.015	12.65	1.0317	0.3964	0.2077	14.7691	− 0.1369	1.0317	0.3766	0.2301	13.8515	− 0.1578
0.020	12.81	1.0704	0.3943	0.2121	13.9092	− 0.1149	1.0748	0.3634	0.2305	14.2313	− 0.1217
0.030	13.01	1.2224	0.4216	0.1982	15.0851	− 0.1044	1.2254	0.4147	0.2061	14.0646	− 0.1132
0.040	13.17	1.4631	0.4953	0.1699	14.6999	− 0.0924	1.4857	0.4854	0.1750	14.7908	− 0.0966
0.050	17.76	1.3277	0.4392	0.1990	14.2739	− 0.1130	1.3530	0.4269	0.2054	14.3650	− 0.1188
0.060	18.15	1.4459	0.5041	0.1696	14.3516	− 0.0948	1.5108	0.5022	0.1656	15.3225	− 0.0913
0.080	18.72	1.6698	0.6218	0.1240	14.3394	− 0.0710	2.0271	0.5024	0.1895	12.3155	− 0.0967
0.100	19.12	1.8417	0.7511	0.0789	14.3264	− 0.0511	2.4921	0.6323	0.1350	12.4641	− 0.0915
0.150	19.77	2.0810	0.9617	0.0208	13.6923	− 0.0265	3.2826	0.8855	0.0469	13.4223	− 0.0480
0.200	20.23	2.1605	1.1091	− 0.0100	12.6080	− 0.0194	3.4458	1.0597	0.0054	12.8999	− 0.0334
0.300	20.73	2.1725	1.2349	− 0.0349	10.4784	− 0.0123	3.1533	1.2404	− 0.0349	10.5530	− 0.0138
0.400	21.03	2.1375	1.2775	− 0.0432	9.9441	− 0.0100	2.8432	1.3192	− 0.0531	24.2566	0.0109
0.500	21.26	2.0906	1.2891	− 0.0459	8.6239	− 0.0100	2.6176	1.3439	− 0.0593	15.4693	0.0064
0.600	21.39	2.0297	1.3110	− 0.0541	19.6967	0.0087	2.4793	1.3326	− 0.0581	18.4681	0.0098
0.800	21.38	1.9485	1.2993	− 0.0544	16.1709	0.0096	2.2628	1.3192	− 0.0584	14.1964	0.0090
1.000	21.53	1.8863	1.2781	− 0.0538	17.7844	0.0154	2.1293	1.2905	− 0.0562	16.9103	0.0152
1.500	16.27	1.8294	1.2144	− 0.0439	16.1327	0.0130	1.9387	1.2323	− 0.0486	14.8470	0.0164
2.000	13.02	1.7808	1.1530	− 0.0320	15.3053	0.0091	1.8351	1.1599	− 0.0340	14.8788	0.0107
3.000	12.14	1.6739	1.0630	0.0096	15.6486	− 0.0022	1.6957	1.0607	− 0.0119	14.1922	0.0002
4.000	11.93	1.5985	0.9967	0.0051	13.0096	− 0.0091	1.6075	0.9914	0.0062	14.3753	− 0.0095
5.000	11.87	1.5377	0.9429	0.0230	10.8137	− 0.0215	1.5481	0.9251	0.0277	12.9752	− 0.0258
6.000	11.82	1.4857	0.9305	0.0252	11.9012	− 0.0202	1.4749	0.9290	0.0248	15.5150	− 0.0283
8.000	11.79	1.4052	0.9020	0.0338	13.7846	− 0.0280	1.3816	0.9078	0.0322	12.0254	− 0.0231
10.000	11.76	1.3432	0.8837	0.0415	13.1135	− 0.0333	1.3125	0.9124	0.0306	14.4197	− 0.0258
15.000	11.74	1.2555	0.8410	0.0587	14.2675	− 0.0524	1.2295	0.8560	0.0530	14.2998	− 0.0306

5 Conclusion

The glass system of $(59.5-x)P_2O_5$–$30Na_2O10Al_2O_3$–$0.5CoO$–xNd_2O_3, where $x = 1$, 2, 3, 4 and 5 (mol%), has been successfully fabricated with the help of the melt quenching technique to indicate gamma shielding properties. Al_20_5, Na_2O and CoO ratios were kept constant and the effect of Nd_2O_3 ratio, which increased with partial decrease of P_2O_5 ratio, on the shielding properties of glass samples was investigated. The theoretical values of the mass attenuation coefficient were calculated using the XCOM program at 356-keV and 662-keV photon energy values with XCOM program. X-ray diffraction (XRD) was characterized for fabricated glasses. The μ_m values of the samples were measured using the NaI (T1) scintillation detector. Z_{eff}, HVL, MFP, EBF and EABF gamma shielding parameters were calculated to examine the gamma radiation shielding features of ND1, ND2, ND3, ND4 and ND5 glass samples. The results highlighted that both the μ_m and Z_{eff} values increased as the Nd_2O_3 concentration increased. On the other hand, HVL, MFP, EBF and EABF values decreased as the Nd_2O_3 concentration increased. ND5 glass has the lowest HVL, MFP, EBF and EABF values. Finally, the mass attenuation coefficient comparison has been done between experimental results and XCOM program. Theoretical and experimental data of μ_m values are highly compatible and supportive indicating the distinctive protection ability to attenuate photon radiation of ND5 glass sample. Thus, glass samples prepared have been shown to reduce the harmful effects of radiation. The data achieved from this study can be useful for further research on the use of glass materials, a new generation material, in efficient and environmentally friendly shielding applications. The different comprehensive measurements can be performed between traditional lead shields and studied glasses considering the significant parameters such as production cost, environmental effects, toxicity, durability. Hereby, it should be noted that continuous efforts on further improvements are necessary.

Table 6 (EBF and EABF) G-P fitting coefficients (b, c, a, X_k and d) of ND4 glass sample

E (MeV)	Z_{eq}	EBF					EABF				
		b	c	a	X_k	d	b	c	a	X_k	d
0.015	12.95	1.0293	0.3943	0.2062	15.4155	− 0.1386	1.0293	0.3656	0.2387	14.0858	− 0.1688
0.020	13.14	1.0646	0.3902	0.2140	14.3739	− 0.1185	1.0689	0.3603	0.2319	14.7491	− 0.1250
0.030	13.39	1.2056	0.4113	0.2051	14.6598	− 0.1090	1.2078	0.4071	0.2096	14.1948	− 0.1146
0.040	13.57	1.4248	0.4780	0.1788	14.5185	− 0.0993	1.4441	0.4705	0.1819	14.7021	− 0.1007
0.050	18.97	1.2702	0.4087	0.2166	14.2008	− 0.1271	1.2903	0.4006	0.2178	14.8353	− 0.1280
0.060	19.42	1.3678	0.4715	0.1839	14.3133	− 0.1038	1.4217	0.4592	0.1871	14.7873	− 0.1056
0.080	20.04	1.5619	0.5733	0.1423	14.3509	− 0.0802	1.7382	0.5721	0.1364	15.8448	− 0.0740
0.100	20.47	1.7273	0.6947	0.0975	14.2833	− 0.0599	2.1499	0.6673	0.1060	15.8846	− 0.0713
0.150	21.21	1.9723	0.9030	0.0363	13.7860	− 0.0324	3.0613	0.8069	0.0733	13.7705	− 0.0655
0.200	21.71	2.0702	1.0534	0.0023	12.7827	− 0.0234	3.2889	0.9834	0.0263	12.9617	− 0.0443
0.300	22.09	2.1163	1.1955	− 0.0276	10.8674	− 0.0140	3.1200	1.1823	− 0.0223	11.0928	− 0.0200
0.400	22.55	2.0896	1.2478	− 0.0378	10.1993	− 0.0113	2.8366	1.2681	− 0.0422	20.1199	0.0004
0.500	22.72	2.0497	1.2729	− 0.0436	8.5300	− 0.0091	2.6204	1.3046	− 0.0509	13.7653	− 0.0001
0.600	22.86	2.0014	1.2891	− 0.0493	15.7658	0.0025	2.4816	1.3013	− 0.0512	15.7848	0.0026
0.800	23.03	1.9324	1.2742	− 0.0482	13.0514	0.0018	2.2682	1.2896	− 0.0510	11.9682	0.0008
1.000	23.06	1.8698	1.2678	− 0.0517	18.4063	0.0149	2.1295	1.2779	− 0.0536	17.4535	0.0141
1.500	17.92	1.8147	1.2111	− 0.0430	16.2642	0.0125	1.9428	1.2224	− 0.0461	15.0605	0.0147
2.000	13.76	1.7733	1.1545	− 0.0328	14.7430	0.0098	1.8373	1.1562	− 0.0332	14.4515	0.0102
3.000	12.64	1.6734	1.0595	− 0.0019	12.7850	− 0.0024	1.6947	1.0597	− 0.0114	12.1575	− 0.0006
4.000	12.37	1.6015	0.9882	0.0081	12.7133	− 0.0119	1.6062	0.9920	0.0060	13.8005	− 0.0091
5.000	12.26	1.5356	0.9453	0.0224	10.3649	− 0.0200	1.5447	0.9281	0.0269	13.3271	− 0.0260
6.000	12.16	1.4835	0.9338	0.0243	12.0638	− 0.0200	1.4723	0.9302	0.0248	15.3578	− 0.0286
8.000	12.13	1.4038	0.9040	0.0335	13.8540	− 0.0282	1.3792	0.9095	0.0319	12.2486	− 0.0236
10.000	12.08	1.3413	0.8873	0.0408	13.0850	− 0.0332	1.3089	0.9168	0.0296	14.5476	− 0.0255
15.000	12.07	1.2523	0.8487	0.0565	14.2921	− 0.0508	1.2308	0.8431	0.0585	14.1631	− 0.0522

Table 7 (EBF and EABF) G-P fitting coefficients (b, c, a, X_k and d) of ND5 glass sample

E (MeV)	Z_{eq}	EBF					EABF				
		b	c	a	X_k	d	b	c	a	X_k	d
0.015	13.26	1.0274	0.3818	0.2212	14.5531	− 0.1497	1.0271	0.3778	0.2264	13.3176	− 0.1452
0.020	13.47	1.0593	0.4042	0.2003	15.6520	− 0.1143	1.0619	0.3860	0.2112	15.8804	− 0.1183
0.030	13.74	1.1902	0.4019	0.2114	14.2732	− 0.1132	1.1917	0.4001	0.2127	14.3133	− 0.1160
0.040	13.94	1.3902	0.4624	0.1868	14.3548	− 0.1056	1.4067	0.4570	0.1881	14.6221	− 0.1043
0.050	20.04	1.2250	0.4047	0.2131	14.1390	− 0.1173	1.2390	0.3887	0.2251	14.2213	− 0.1325
0.060	20.52	1.3167	0.4510	0.1936	14.2422	− 0.1110	1.3610	0.4424	0.1938	14.7632	− 0.1088
0.080	21.18	1.4990	0.5512	0.1503	14.3785	− 0.0839	1.6532	0.5443	0.1480	15.6879	− 0.0814
0.100	21.65	1.6479	0.6624	0.1084	14.2426	− 0.0644	2.0208	0.6243	0.1229	15.6769	− 0.0792
0.150	22.42	1.8871	0.8594	0.0479	13.8771	− 0.0365	2.8870	0.7461	0.0945	14.1030	− 0.0800
0.200	22.93	1.9997	1.0100	0.0120	12.9191	− 0.0264	3.1663	0.9238	0.0427	13.0100	− 0.0527
0.300	23.45	2.0638	1.1587	− 0.0208	11.2310	− 0.0155	3.0889	1.1280	− 0.0104	11.5973	− 0.0258
0.400	23.84	2.0516	1.2241	− 0.0336	10.4022	− 0.0123	2.8313	1.2276	− 0.0336	16.8318	− 0.0079
0.500	24.07	2.0144	1.2588	− 0.0416	8.4489	− 0.0084	2.6228	1.2706	− 0.0437	12.2953	− 0.0057
0.600	24.24	1.9767	1.2700	− 0.0451	12.3307	− 0.0030	2.4836	1.2739	− 0.0452	13.4398	− 0.0037
0.800	24.38	1.9200	1.2549	− 0.0434	10.6503	− 0.0042	2.2723	1.2668	− 0.0454	10.2531	− 0.0055
1.000	24.33	1.8569	1.2599	− 0.0500	18.8908	0.0145	2.1297	1.2681	− 0.0515	17.8766	0.0132
1.500	18.63	1.8076	1.2129	− 0.0436	15.6261	0.0129	1.9404	1.2220	− 0.0460	14.9807	0.0144
2.000	14.73	1.7651	1.1557	− 0.0330	14.8646	0.0099	1.8373	1.1550	− 0.0330	13.5614	0.0100
3.000	13.06	1.6727	1.0571	− 0.0100	10.7671	− 0.0025	1.6943	1.0585	− 0.0108	10.7935	− 0.0013
4.000	12.73	1.6046	0.9801	0.0109	12.4309	− 0.0145	1.6055	0.9920	0.0060	13.1934	− 0.0089
5.000	12.62	1.5324	0.9510	0.0202	10.6266	− 0.0179	1.5390	0.9364	0.0240	13.7393	− 0.0242
6.000	12.54	1.4824	0.9335	0.0251	12.1845	− 0.0218	1.4685	0.9328	0.0245	15.2182	− 0.0288
8.000	12.45	1.4008	0.9090	0.0321	13.8639	− 0.0274	1.3772	0.9109	0.0315	12.9772	− 0.0249
10.000	12.41	1.3387	0.8926	0.0398	13.0651	− 0.0332	1.3086	0.9122	0.0319	14.4578	− 0.0279
15.000	12.40	1.2493	0.8561	0.0541	14.5166	− 0.0497	1.2298	0.8395	0.0605	14.1765	− 0.0545

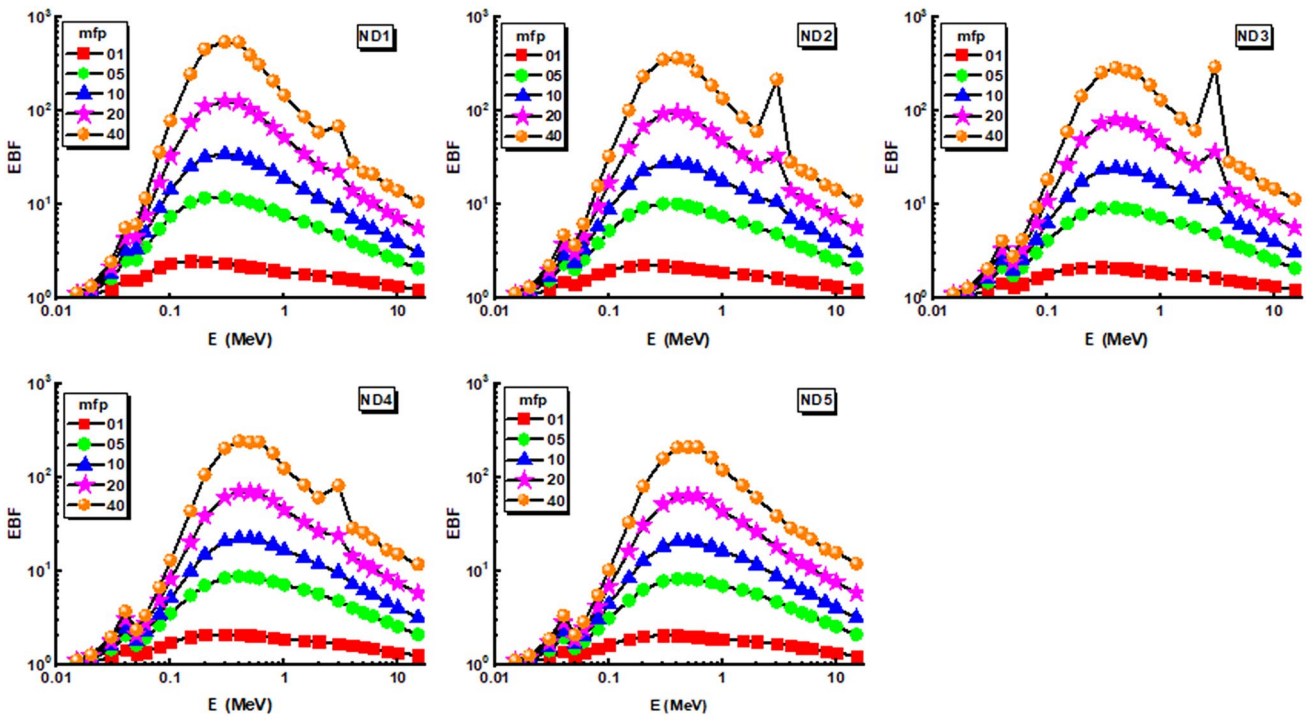

Fig. 7 Exposure buildup factor (EBF) against photon energy of glass samples at 1, 5, 10, 20 and 40 mfp

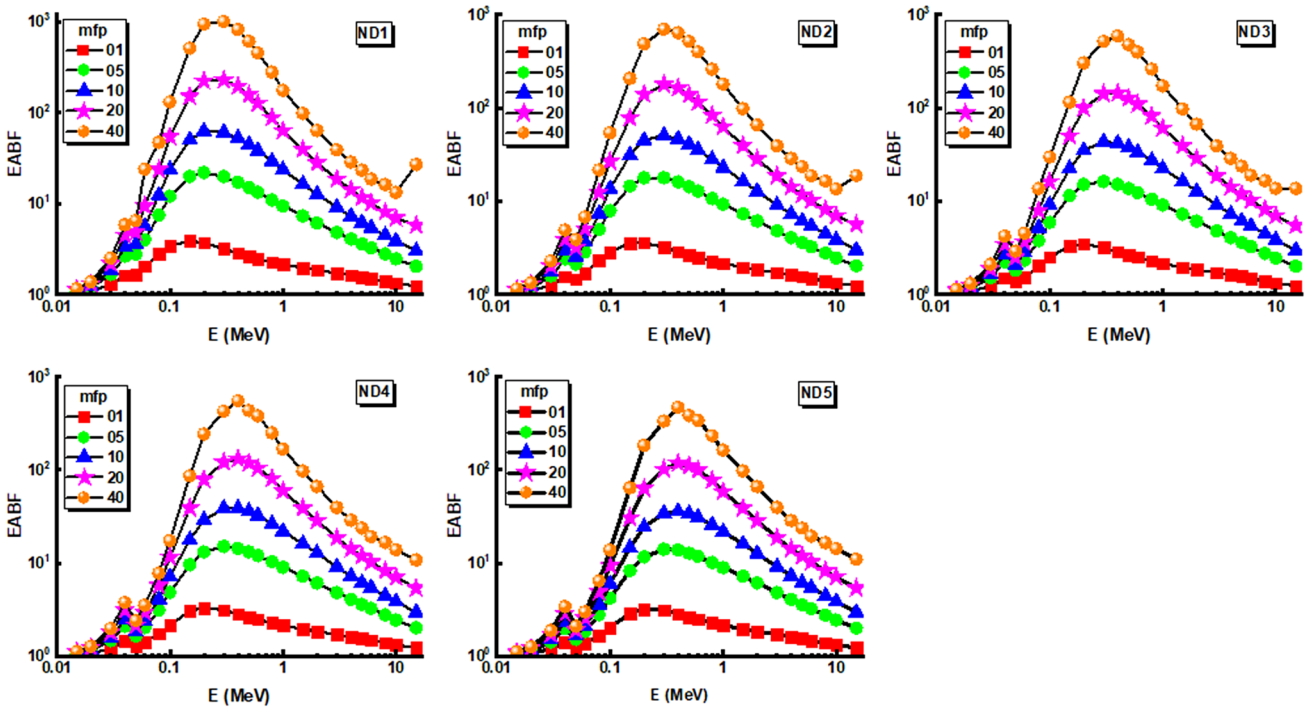

Fig. 8 Energy absorption buildup factor (EABF) against photon energy of glass samples at 1, 5, 10, 20 and 40 mfp

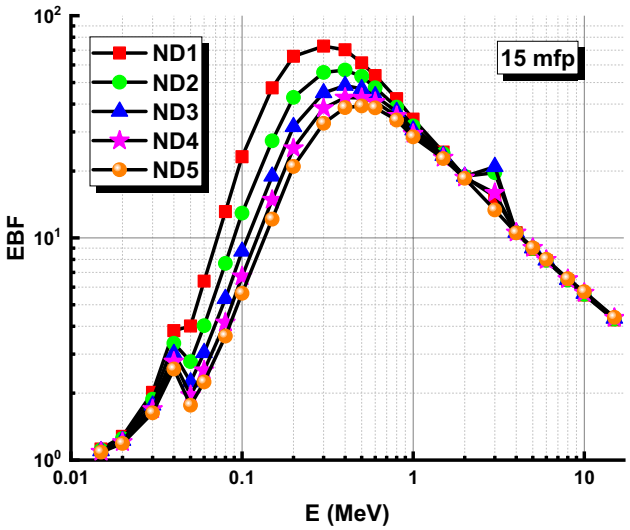

Fig. 9 Exposure buildup factor (EBF) against photon energy of glass samples at 15 mfp

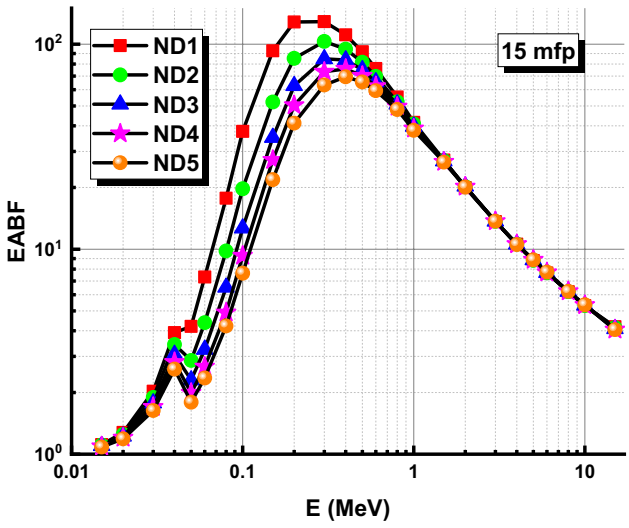

Fig. 10 Energy absorption buildup factor (EABF) against photon energy of glass samples at 15 mfp

References

1. H.E. Hassan, H.M. Badran, A. Aydarous, T. Sharshar, Studying the effect of nano lead compounds additives on the concrete shielding properties for γ-rays. Nucl. Instrum. Methods Phys. Res. Sect. B Beam Interact Mater. Atoms **360**, 81–89 (2015). https://doi.org/10.1016/j.nimb.2015.07.126
2. A.S. Wagh, S.Y. Sayenko, A.N. Dovbnya, V.A. Shkuropatenko, R.V. Tarasov, A.V. Rybka, A.A. Zakharchenko, Durability and shielding performance of borated ceramicrete coatings in beta and gamma radiation fields. J. Nucl. Mater. **462**, 165–172 (2015). https://doi.org/10.1016/j.jnucmat.2015.03.049
3. D.K. Gaikwad, M.I. Sayyed, S.S. Obaid, S.A.M. Issa, P.P. Pawar, Gamma ray shielding properties of TeO_2–ZnF_2–As_2O_3–Sm_2O_3

glasses. J. Alloys Compd. **765**, 451–458 (2018). https://doi.org/10.1016/j.jallcom.2018.06.240
4. O. Agar, Z.Y. Khattari, M.I. Sayyed, H.O. Tekin, S. Al-Omari, M. Maghrabi, M.H.M. Zaid, I.V. Kityk, Evaluation of the shielding parameters of alkaline earth based phosphate glasses using MCNPX code. Results Phys. **12**, 101–106 (2019). https://doi.org/10.1016/j.rinp.2018.11.054
5. O. Agar, H.O. Tekin, M.I. Sayyed, M.E. Korkmaz, O. Culfa, C. Ertugay, Experimental investigation of photon attenuation behaviors for concretes including natural perlite mineral. Results Phys. **12**, 237–243 (2019). https://doi.org/10.1016/j.rinp.2018.11.053
6. H.O. Tekin, E.E. Altunsoy, E. Kavaz, M.I. Sayyed, O. Agar, M. Kamislioglu, Photon and neutron shielding performance of boron phosphate glasses for diagnostic radiology facilities. Results Phys. **12**, 1457–1464 (2019). https://doi.org/10.1016/j.rinp.2019.01.060
7. M.G. Dong, O. Agar, H.O. Tekin, O. Kilicoglu, K.M. Kaky, M.I. Sayyed, A Comparative study on gamma photon shielding features of various germanate glass systems. Compos. Part B Eng. **165**, 636–647 (2019). https://doi.org/10.1016/j.compositesb.2019.02.022
8. A. Sharma, M.I. Sayyed, O. Agar, H.O. Tekin, Simulation of shielding parameters for TeO_2–WO_3–GeO_2 glasses using FLUKA code. Results Phys. **13**, 102199 (2019). https://doi.org/10.1016/j.rinp.2019.102199
9. S. Tuscharoen, J. Kaewkhao, P. Limkitjaroenporn, P. Limsuwan, W. Chewpraditkul, Improvement of BaO:B_2O_3: fly ash glasses: radiation shielding, physical and optical properties. Ann. Nucl. Energy **49**, 109–113 (2012). https://doi.org/10.1016/j.anucene.2012.05.017
10. S.R. Manohara, S.M. Hanagodimath, L. Gerward, Photon interaction and energy absorption in glass: a transparent gamma ray shield. J. Nucl. Mater. **393**, 465–472 (2009). https://doi.org/10.1016/j.jnucmat.2009.07.001
11. C. Bootjomchai, J. Laopaiboon, C. Yenchai, R. Laopaiboon, Gamma-ray shielding and structural properties of barium-bismuth-borosilicate glasses. Radiat. Phys. Chem. **81**, 785–790 (2012). https://doi.org/10.1016/j.radphyschem.2012.01.049
12. S.P. Edirisinghe, C.A. Hogarth, Optical properties of some copper phosphate glasses containing calcium and barium. J. Mater. Sci. Lett. **8**, 789–792 (1989). https://doi.org/10.1007/bf01730139
13. M.A. Karakassides, A. Saranti, I. Koutselas, Preparation and structural study of binary phosphate glasses with high calcium and/or magnesium content. J. Non-Cryst. Solids **347**, 69–79 (2004). https://doi.org/10.1016/j.jnoncrysol.2004.08.111
14. A. Mogus-Milankovic, A. Gajovic, A. Santic, D.E. Day, Structure of sodium phosphate glasses containing Al_2O_3 and/or Fe_2O_3. Part I. J. Non-Cryst. Solids **289**, 204–213 (2001). https://doi.org/10.1016/S0022-3093(01)00701-3
15. J. Yifen, J. Dehua, C. Xiangsheng, B. Beiya, H. Xihuai, Raman spectrum studies of the glasses in the system Na_2O–Al_2O_3–P_2O_5. J. Non-Cryst. Solids **80**, 147–151 (1986). https://doi.org/10.1016/0022-3093(86)90388-1
16. S.M. Abo-Naf, N.A. Ghoneim, H.A. Ei-Batal, Preparation and characterization of solegel derived glasses in the ternary Na_2O–Al_2O_3–P_2O_5 system. J. Mater. Sci. Mater. Electron. **15**, 273–282 (2004). https://doi.org/10.1023/B:JMSE.0000024226.51362.de
17. Y. Yue, Y. Wang, Y. Cao, S. Chen, Q. Zhou, W. Chen, L. Hu, Effect of Al_2O_3 on structure and properties of Al_2O_3–K_2O–P_2O_5 glasses. Opt. Mater. Express **8**, 245–258 (2018). https://doi.org/10.1364/OME.8.000245
18. Y.B. Saddeek, M.A. Kaid, M.R. Ebeid, FTIR and physical features of Al_2O_3–La_2O_3–P_2O_5–PbO glasses. J. Non-Cryst. Solids **387**, 30–35 (2014). https://doi.org/10.1016/j.jnoncrysol.2013.12.029
19. A. Faivre, F. Despetis, L. Duffours, P. Colombel, Effect of CaO and Al_2O_3 addition on the properties of K_2O–Na_2O–P_2O_5 glass system. Int. J. Appl. Glass Sci. **10**, 162–171 (2019). https://doi.org/10.1111/ijag.13066
20. D. Manzani, J.B. Souza Junior, A.S. Reyna, M.L. Silva Neto, J.E.Q. Bautista, S.J.L. Ribeiro, C.B. de Araújo, Phosphotellurite glass and glass-ceramics with high TeO_2 contents: thermal, structural and optical properties. Dalton Trans. **48**, 6261–6272 (2019). https://doi.org/10.1039/C9DT00691E
21. A.K. Yadav, P. Singh, A review of the structures of oxide glasses by Raman spectroscopy. RSC Adv. **5**, 67583–67609 (2015). https://doi.org/10.1039/C5RA13043C
22. A. Langar, N. Sdiri, H. Elhouichet, M. Ferid, Structure and electrical characterization of ZnO–Ag phosphate glasses. Results Phys. **7**, 1022–1029 (2017). https://doi.org/10.1016/j.rinp.2017.02.028
23. Q. Yin, S. Kang, X. Wang, S. Li, D. He, L. Hu, Effect of PbO on the spectral and thermo-optical properties of Nd_3 p-doped phosphate laser glass. Opt. Mater. **66**, 23–28 (2017). https://doi.org/10.1016/j.optmat.2017.01.036
24. M.K. Narayanan, H.D. Shashikala, Thermal and optical properties of BaO–CaF_2–P_2O_5 glasses. J. Non-Cryst. Solids **422**, 6–11 (2015). https://doi.org/10.1016/j.jnoncrysol.2015.04.038
25. H.O. Tekin, L.R.P. Kassab, S.A.M. Issa, C.D.S. Bordon, E.E. Altunsoy Guclu, G.R. da Silva Mattos, O. Kilicoglu, Synthesis and nuclear radiation shielding characterization of newly developed germanium oxide and bismuth oxide glasses. Ceram. Int. (2019). https://doi.org/10.1016/j.ceramint.2019.08.204
26. M.I. Sayyed, S.A.M. Issa, H.O. Tekin, Y.B. Saddeek, Comparative study of gamma-ray shielding and elastic properties of BaO–Bi_2O_3–B_2O_3 and ZnO–Bi_2O_3–B_2O_3 glass systems. Mater. Chem. Phys. (2018). https://doi.org/10.1016/j.matchemphys.2018.06.034
27. N. Chanthima, J. Kaewkhao, Investigation on radiation shielding parameters of bismuth borosilicate glass from 1 keV to 100 GeV. Ann. Nucl. Energy **55**, 23–28 (2013). https://doi.org/10.1016/j.anucene.2012.12.011
28. M.I. Sayyed, S.A.M. Issa, S.H. Auda, Assessment of radio-protective properties of some anti-inflammatory drugs. Prog. Nucl. Energy **100**, 297–308 (2017). https://doi.org/10.1016/j.pnucene.2017.07.003
29. S.A.M. Issa, M.I. Sayyed, M.H.M. Zaid, K.A. Matori, Photon parameters for gamma-rays sensing properties of some oxide of lanthanides. Results Phys. **9**, 206–210 (2018). https://doi.org/10.1016/j.rinp.2018.02.039
30. A.A.A. Darwish, S.A.M. Issa, M.M. El-Nahass, Effect of gamma irradiation on structural, electrical and optical properties of nanostructure thin films of nickel phthalocyanine. Synth. Met. **215**, 200–206 (2016). https://doi.org/10.1016/j.synthmet.2016.03.002
31. S.A.M. Issa, A.A.A. Darwish, M.M. El-Nahass, The evolution of gamma-rays sensing properties of pure and doped phthalocyanine. Prog. Nucl. Energy. **100**, 276–282 (2017). https://doi.org/10.1016/j.pnucene.2017.06.016
32. P. Sathiyaraj, E.J.J. Samuel, C.C.S. Valeriano, M. Kurudirek, Effective atomic number and buildup factor calculations for metal nano particle doped polymer gel. Vacuum **143**, 138–149 (2017). https://doi.org/10.1016/j.vacuum.2017.06.005
33. S.A.M. Issa, H.O. Tekin, T.T. Erguzel, G. Susoy, The effective contribution of PbO on nuclear shielding properties of xPbO–(100–x)P_2O_5 glass system: a broad range investigation. Appl. Phys. A **125**, 640 (2019). https://doi.org/10.1007/s00339-019-2941-x
34. S.A.M. Issa, H.O. Tekin, The multiple characterization of gamma, neutron and proton shielding performances of xPbO–(99–x)B_2O_3–Sm_2O_3 glass system. Ceram. Int. **45**, 23561–23571 (2019). https://doi.org/10.1016/j.ceramint.2019.08.065
35. M. Kurudirek, S. Topcuoglu, Investigation of human teeth with respect to the photon interaction, energy absorption and buildup

factor. Nucl. Instru. Methods Phys Res. Sect. B Beam Interact Mater. Atoms **269**, 1071–1081 (2011). https://doi.org/10.1016/j.nimb.2011.03.004

36. V.P. Singh, N.M. Badiger, Energy absorption buildup factors, exposure buildup factors and Kerma for optically stimulated luminescence materials and their tissue equivalence for radiation dosimetry. Radiat. Phys. Chem. **104**, 61–67 (2014). https://doi.org/10.1016/j.radphyschem.2013.11.025
37. Y. Karabul, L. Amon Susam, O. İçelli, Ö. Eyecioğlu, Computation of EABF and EBF for basalt rock samples. Nucl. Instrum. Methods Phys. Res. Sect. A Accel. Spectrom. Detect. Assoc. Equip. **797**, 29–36 (2015). https://doi.org/10.1016/j.nima.2015.06.024
38. I.S. Mahmoud, S.A.M. Issa, Y.B. Saddeek, H.O. Tekin, O. Kilicoglu, T. Alharbi, M.I. Sayyed, T.T. Erguzel, R. Elsaman, Gamma, neutron shielding and mechanical parameters for lead vanadate glasses. Ceram. Int. (2019). https://doi.org/10.1016/j.ceramint.2019.04.105
39. S.A.M. Issa, A.M.A. Mostafa, T.A. Hanafy, M. Dong, X. Xue, Comparison study of photon attenuation characteristics of poly vinyl alcohol (PVA) doped with $Pb(NO_3)_2$ by MCNP5 code, XCOM and experimental results. Prog. Nucl. Energy **111**, 15–23 (2019). https://doi.org/10.1016/j.pnucene.2018.10.018
40. M.J. Berger, J.H. Hubbell, S.M. Seltzer, J. Chang, J.S. Coursey, R. Sukumar, D.S. Zucker, K. Olsen, XCOM: photon cross section database (version 1.5). National Institute of Standards and Technology, Gaithersburg, MD (2010). http://physics.nist.gov/xcom. Accessed 8 June 2020
41. R. Divina, K. Marimuthu, M.I. Sayyed, H.O. Tekin, O. Agar, Physical, structural, and radiation shielding properties of B_2O_3–MgO–K_2O–Sm_2O_3 glass network modified with TeO_2. Radiat. Phys. Chem. **160**, 75–82 (2019). https://doi.org/10.1016/j.radphyschem.2019.03.029
42. E. Kavaz, H.O. Tekin, O. Agar, E.E. Altunsoy, O. Kilicoglu, M. Kamislioglu, M.M. Abuzaid, M.I. Sayyed, The Mass stopping power/projected range and nuclear shielding behaviors of barium bismuth borate glasses and influence of cerium oxide. Ceram. Int. **45**, 15348–15357 (2019). https://doi.org/10.1016/j.ceramint.2019.05.028
43. H.O. Tekin, E. Kavaz, E.E. Altunsoy, M. Kamislioglu, O. Kilicoglu, O. Agar, M.I. Sayyed, N. Tarhan, Characterization of a broad range gamma-ray and neutron shielding properties of MgO–Al_2O_3–SiO_2–B_2O_3 and Na_2O–Al_2O_3–SiO_2 glass systems. J. Non-Cryst. Solids **518**, 92–102 (2019). https://doi.org/10.1016/j.jnoncrysol.2019.05.012
44. H.O. Tekin, E. Kavaz, A. Papachristodoulou, M. Kamislioglu, O. Agar, E.E. Altunsoy Guclu, O. Kilicoglu, M.I. Sayyed, Characterization of SiO2–PbO–CdO–Ga_2O_3 glasses for comprehensive nuclear shielding performance: alpha, proton, gamma, neutron. Radiat. Ceram. Int. **45**, 19206–19222 (2019). https://doi.org/10.1016/j.ceramint.2019.06.168
45. S.A.M. Issa, G. Susoy, A.M. Ali, H.O. Tekin, Y.B. Saddeek, A. Al-Hajry, H. Algarni, P.S. Anjana, O. Agar, The effective role of La_2O_3 contribution on zinc borate glasses: radiation shielding and mechanical properties. Appl. Phys. A **125**, 867 (2019). https://doi.org/10.1007/s00339-019-3169-5
46. M.R. Kacal, H. Polat, M. Oltulu, F. Akman, O. Agar, H.O. Tekin, Gamma shielding and compressive strength analyses of polyester composites reinforced with zinc: an experiment, theoretical, and simulation based study. Appl. Phys. A **126**, 205 (2020). https://doi.org/10.1007/s00339-020-3382-2
47. M.S. Al-Buriahi, H.O. Tekin, E. Kavaz, B.T. Tonguc, Y.S. Rammah, New transparent rare earth glasses for radiation protection applications. Appl. Phys. A **125**, 866 (2019). https://doi.org/10.1007/s00339-019-3077-8
48. S.A.M. Issa, Y.B. Saddeek, M.I. Sayyed, H.O. Tekin, O. Kilicoglu, Radiation shielding features using MCNPX code and mechanical properties of the PbO–Na_2O–B_2O_3–CaO–Al_2O_3–SiO_2 glass systems. Compos. Part B Eng. **167**, 231–240 (2019). https://doi.org/10.1016/j.compositesb.2018.12.029
49. A.S. Abouhaswa, Y.S. Rammah, M.I. Sayyed, H.O. Tekin, Synthesis, structure, optical and gamma radiation shielding properties of B_2O_3–PbO_2–Bi_2O_3 glasses. Compos. B **172**, 218–225 (2019). https://doi.org/10.1016/j.compositesb.2019.05.040